Numerical Simulation of the Performance Characteristics of the Hybrid Closed Circuit Cooling Tower

M. M. A. Sarker[1], E. Kim[2], C. G. Moon[2], J. I. Yoon[2]

[1]Department of Mathematics
Bangladesh University of Engineering and Technology
Dhaka-1000, Bangladesh
masarker@math.buet.ac.bd

[2]Department of Refrigeration and Air-conditioning Engineering
Pukyong National University
Namgu, Pusan 608-739, Korea

Received: 15.05.2007 **Revised:** 01.12.2007 **Published online:** 06.03.2008

Abstract. The performance characteristics of the Hybrid Closed Circuit Cooling Tower (HCCCT) have been investigated applying computational fluid dynamics (CFD). Widely reported CFD techniques are applied to simulate the air-water two phase flow inside the HCCCT. The pressure drop and the cooling capacity were investigated from several perspectives. Three different transverse pitches were tested and found that a pitch of 45 mm had lower pressure drop. The CFD simulation indicated that when air is supplied from the side wall of the HCCCT, the pressure drop can be over predicted and the cooling capacity can be under predicted mainly due to the non-uniform air flow distribution across the coil bank. The cooling capacity in wet mode have been calculated with respect to wet-bulb temperature (WBT) and cooling water to air mass flow rates for different spray water volume flow rates and the results were compared to the experimental measurement and found to conform well for the air supply from the bottom end. The differences of the cooling capacity and pressure drop in between the CFD simulation and experimental measurement in hybrid mode were less than 5 % and 7 % respectively for the uniform air flow distribution.

Keywords: hybrid closed circuit cooling tower, wet-bulb temperature, wet mode operation, dry mode operation, cooling capacity.

1 Introduction

Cooling towers are used to reject heat, cool buildings and reduce the temperature of water circulated through various heat rejection equipments. When evaporative cooling is produced, cooling towers are called wet tower whereas known as dry tower when air blast cooling is utilized. The HCCCT is a closed circuit cooling tower which is capable of working both in wet mode and in dry mode. Cooling or condensing system for fluids operates as a dry cooler in winter and as an evaporative cooler in summer by spraying on the heat transfer surface [1]. HCCCT works well in dry mode during the mid-season and winter as long as ambient temperature remains below $12–14$ °C, no plume and no freezing and lower noise levels are ensured in the dry mode operation. HCCCT operates smoothly in wet mode while the ambient temperature goes above $12–14$ °C, water consumption by HCCCT is lower than those of Wet Closed Cooling Tower (WCCT) and the process water can be cooled down to 4 °C above the wet-bulb temperature and can be packed in light and compact bundle with optimized circuitry [2]. In the HCCCT, water is sprayed in summer using spray nozzles from the top along with a counter-type of air flow in both summer and winter from the bottom end. Pressure drop is an aspect which is directly related to the economic operation of the cooling tower and will be investigated along with the cooling capacity.

The objective of present study is to investigate cooling effect and pressure drop of HCCCT due to the variations of the coil's transverse pitch, location of the air inlet, air inlet velocity and temperature as well as for different flow rates of cooling water and spray water and, to demonstrate the validity of the numerical simulation comparing the results with the experimental data for the prototype HCCCT. The work involves the prediction of the performances in dry mode during the winter season and at the wet mode in summer.

2 Previous studies

The basic theory of cooling tower operation was first proposed by Walker et al. [3]. Merkel [4] combined the heat and water vapor transfer related differential equations in an evaporative cooling tower using a number of simplifying assumptions. Fisenko et al. [5] presented a mathematical model of the performance of a cooling tower consisting of two interdependent boundary-value problems, including 9 ODE and an algorithm of self-consistent solution. Jameel-Ur-Rehman et al. [6] reported a model of counter flow wet cooling towers, where they verified the authenticity of the model comparing the values of number of transfer units (NTU) and tower effectiveness with the commonly described models. Ala Hasan et al. [7] presented the theoretical analysis and computational modeling of closed wet cooling towers. Jaber et al. [8] incorporated the effectiveness and NTU definitions for heat exchanger design with those to the cooling tower operating conditions. Mizushima et al. [9] reported design equations for an evaporative cooler, where fluid inside the tube is cooled by utilizing the latent heat of vaporization. Optimum utilization of the CFD for predicting the thermal performance of closed wet cooling towers are reported by number authors including Gan et al. [10–12]. This review indicates that numerical results about performance characteristics of HCCCT is lacking.

3 Experimental details of the prototype HCCCT

The dimension of prototype forced draft HCCCT is 1.04 m $\times$ 2.36 m $\times$ 3.2 m with a rated capacity of 30 RT. The copper coils having 15.88 mm of outer diameter were used in the heat exchanger in staggered arrangement in 16 rows and 22 columns. The transverse pitch was 45 mm and the length of each coil was 2.34 m. The performance of the HCCCT was experimentally tested at Daeil Aqua [13]. The maximum cooling capacities in dry and wet modes at the designed conditions were 32 Mcal/h (37 kW in SI) and 29.7 RT (104 kW in SI) and the pressure drops were 2.3 mmAq and 3.9 mmAq respectively.

4 Mathematical models

The cooling capacity of the HCCCT mainly depends on the design parameters and on the operating conditions. A commercial CFD software Fluent [14] is applied to simulate the air-water droplet's two-phase flow. In the numerical simulation, air flow is modeled as a continuous phase and is solved using the Eulerian approach. Water droplets are modeled as the dispersed phase and Lagrangian approach is utilized to solve the water droplet trajectory equations. The transport phenomenon between the two phases is coupled to incorporate the impact of the dispersed phase on the continuous phase. Details can be found from Gan et al. [10–12], Hasan et al. [7].

4.1 Dry mode operation of the HCCCT

The transport equation of air includes the conservation equations for mass, momentum, energy and turbulence. Among turbulence models namely, Standard $k-\varepsilon$ model, RNG (Renormalization Group) model and RSM (Reynolds Stress equation Models), standard $k-\varepsilon$ model is the simplest, widely validated and proven to produce better performance especially for the current simulation and, is applied for predicting the turbulence effect. The model equation for the steady state incompressible flow reduces to

$$\nabla\big(\rho\overline{V}\phi - \Gamma_\phi \nabla\phi\big) = S_\phi + S_\phi^p, \tag{1}$$

where ϕ is the flow variable, $\overline{V}$ is the mean air velocity (m/s), ρ is the air density (kg/m^3), k is the turbulent kinetic energy (m^2/s^2), ε is the dissipation rate (m^2/s^3), Γ_ϕ is the diffusion coefficient (Ns/m^2), S_ϕ is the source term for the continuous phase and S_ϕ^p is the source term related to the interaction between the air and the water droplets. Control volume method has been applied for the discretization and SIMPLEC algorithm [15] is applied to handle the problem related to pressure-velocity coupling. Pressure gradient effects for the boundary layers around the coils of the heat exchanger have been taken into account through the enhanced wall treatment option.

4.2 The wet mode operation of the HCCCT

In wet mode operation, the spherical water droplets disseminate in the continuous gas phase. The numerical simulation has been designed to compute the velocity and the trajectories of the dispersed droplets. Utilizing the force balance on the droplet, the trajectory of a dispersed phase water droplet is predicted. Gan et al. [10–12] reported a numerical technique for evaluating the performance of a closed wet cooling tower. The equation of motion for a spherical water droplet can be given by

$$\frac{dr_p}{dt} = V_p, \tag{2}$$

where r_p is the trajectory and V_p is the instantaneous velocity of the droplet (m/s). The force balance relates the droplet inertia to the forces acting on the droplet including the drag force, the buoyancy force, the force needed to accelerate the apparent mass of the droplet relative to gas and the force due to the pressure gradient in the gas surrounding the droplet. The droplet velocity, V_p can be written as

$$\rho_p \frac{dV_p}{dt} = \frac{3}{4}\frac{\rho C_D |V - V_p|}{d_p}(V - V_p) + g(\rho_p - \rho) + \frac{1}{2}\rho \frac{d}{dt}(V - V_p) + \frac{\partial P}{\partial t_p}, \tag{3}$$

where V is the instantaneous local velocity of air (m/s), dp is the droplet diameter (m), p_ρ is the droplet density (kg/m^3) and P is the static pressure of gas (Pa) and C_D is the drag coefficient, a function of the relative Reynolds number.

In the turbulent flows of air, the droplet trajectory is affected by turbulence and the effect is simulated using a stochastic droplet tracking technique, where the instantaneous air phase velocity V is decomposed as $V = \overline{V} + V'$, where $\overline{V}$ is the mean air velocity and is derived from the solution of the gas phase equations. V' is the fluctuating velocity and is sampled randomly from a normal probability distribution of the gas phase velocity. For an isotropic turbulent flow, V' can be given by:

$$V' = \zeta \sqrt{\frac{2k}{3}} r_0, \tag{4}$$

where ζ is a normally distributed random number, k is the turbulent kinetic energy ($\mathrm{m}^2/\mathrm{s}^2$) and r_0 is a unit vector.

4.3 Evaporative cooling of water droplets

In a mechanical draft HCCCT, the radius of droplets is a function of the spray water flow rate and temperature. The size of the water droplet decreases with the increase of the spray water flow rate. For a counter-flow type HCCCT, the maximum and minimum radii of droplets are categorized respectively, by splitting of large droplets and carrying away of small droplets by the air flow. The maximum diameter of the water droplet falling with a relative velocity v can be derived from the equality of the drag force and surface tension force. For non-broken droplets, the radius R can be given by [16, 17]:

$$R \leq 2.3 \frac{\sigma}{\rho_a \nu^2}, \tag{5}$$

where σ is the surface tension of water. In this CFD simulation, the spray water is injected through 6 nozzles and the distribution was such that the horizontal component of the droplet velocity for each nozzle varied in such a way that the spray water could cover the whole width of the coil bank. The mean diameter of the water droplet is estimated from the terminal velocity of the droplets at a mean velocity of air flowing over the coil bank. The air velocity at the inlet remains constant at 3.1 m/s. It has been observed that the temperature of the coils increase a bit with the increase of the iteration due to the assumption of the volumetric heat generation at the heat exchanger. To overcome this difficulty, Gan et al. [11] suggested that a linear heat flux should be distributed over the heat exchanger for a cooling tower having relatively lower cooling water flow rate. In the present simulation, heat flux defined in equation (6) is applied to improve the accuracy of the prediction in HCCCT having higher cooling water flow rate:

$$q_i = \frac{2}{3}\left(\frac{2N+i-2}{2N-1}\right)q_m, \tag{6}$$

where N is the number of coil rows, i is the coil row, q_i is the heat flux for tube row i ($\mathrm{W/m^2}$) and q_m is the mean heat flux. The heat flux given in equation (6) is based on the assumption that for a fixed overall sensible heat transfer, the transfer rate at the top coil row is approximately 1.5 times that of the bottom coil row.

4.4 Simplifying assumptions

Length of the HCCCT is much larger than the corresponding width, so the fluid flow is assumed to be of 2-dimensional. Moreover, due to the geometrical symmetry of the tower, only the one half of the tower with respect to the vertical center line will be used as the computational domain. HCCCT is considered to be an adiabatic device with negligible heat losses or gains from the surroundings and that fluids are incompressible.

The temperature variation of the cooling water flowing inside the tube is a function of the cooling load and the flow rate of the cooling water. The tubes in the heat exchanger become separate entities at the vertical cross-section of the HCCCT and every tube is modeled as a smooth circular solid cylinder with heat generation. The rate of heat transfer from the heat exchanger to the air works as a source of heat generation and it could either be obtained from the total cooling load measured experimentally or from the models of the thermal performance of the HCCCT [7,10–12]. The inlet louver installed at the caching of the tower has an opening of $-45°$ with the horizontal axis. When a water droplet reaches at the tube coil, water droplets reflect as well as changes in its normal and tangential velocities. Water droplets are assumed to reflect perfectly at the side walls as well as on the symmetry plane and when droplets fall down to the water basin, those escape and that the sticking droplet at the top wall is carried over by the air forced by fan. The nominal simulating condition is given in Table 1. Fig. 1 shows the schematic of the HCCCT along with part of the meshed coil bank.

Table 1. The simulating conditions of the HCCCT

Air	Wet-bulb temperature [°C]	27
	Mass flow rate [kg/s]	8.0
Spray water	Volume flow rate [$\mathrm{m^3/h}$]	33
	Temperature [°C]	29.0
Cooling water	Inlet temperature [°C]	37.0
	Volume flow rate [$\mathrm{m^3/h}$]	24

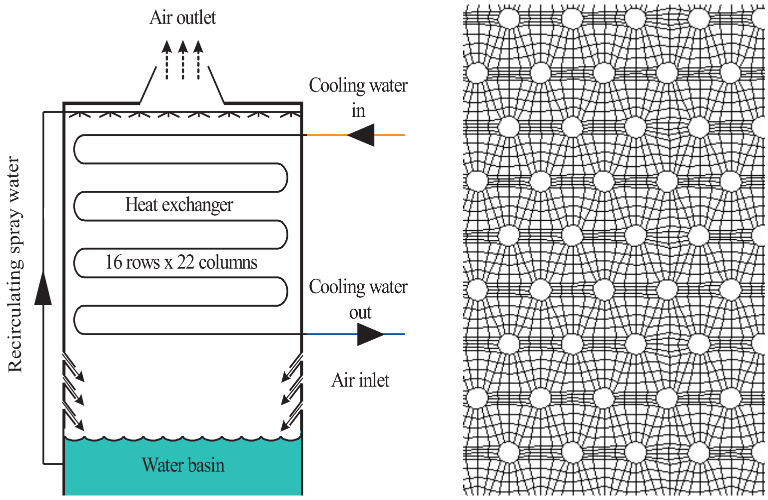

Fig. 1. Schematic and the meshed computational domain of the HCCCT.

5 Results and discussion

5.1 Results on dry mode operation

Pressure drop is one of the prime concerns while dealing with internal flow in pipe or duct because the power required by the pump or fan is directly proportional to the pressure drop. Pressure drop is investigated from three perspectives as discussed next.

The pressure drop at the internal part of the HCCCT is a function of the inlet air velocity. We investigated several cases of pressure drop with respect to (w.r.t.) a variable air inlet velocity ranging from 1.5–4.0 m/s. Comparative pressured drop with a variable inlet air velocity with different air inlet temperature is shown in the left panel of Fig. 2.

The pressure drop across the coil bank is seen to increase with the increase of the inlet air velocity and temperature. At an air velocity of 3.1 m/s and at a temperature of $15\,^\circ$C, the pressured drop is found to be 2.14 mmAq. This could be compared to the experimental pressure drop of 2.3 mmAq. The pressure drop result from the experiment is available for the lower range than that has been investigated in this study as can be inferred from this figure.

The coil pitch plays an important role for increasing/decreasing the rate of the passing air and water flow through heat exchanger in a HCCCT. Too small spacing between the coils can reduce the velocity of the air and water and thereby the heat transfer efficiency could be lower as well. At the air side, more pressure drop causes even more power requirement by the fan. Thus the operational cost gets higher. In the simulation, the pressure distribution having pitches of 32, 40 and 45 mm were investigated. It was found that pressure drops decreased with the increase of the coil's transverse pitches. For all cases, the air velocities at the inlet were kept constant at 3.1 m/s. Right panel of Fig. 2

shows that the coil having higher pitch has lower pressure drop and vice versa and all three cases has similar pressure at the lowest coil due to the constant inlet air flow rate. Coil having a transverse pitch of 45 mm produced lowest pressure drop which was about 2.14 mmAq. Increasing the pitches at will is not a wise idea only for the sake of reducing pressure drop because minimizing the pressure drop and the flow rate of the fluids can minimize operating cost but it can maximize the size of the heat exchanger and thus the initial cost.

The predicted air flow through tube bank having an air inlet velocity of 3.1 m/s and pitch of 45 mm is shown in Fig. 3, where (a) shows the vectors with air supply from the bottom end and that of (b) from the side wall. The air flow inside the heat exchanger could be claimed to be more uniform for the air supply from the bottom end than that from the side wall.

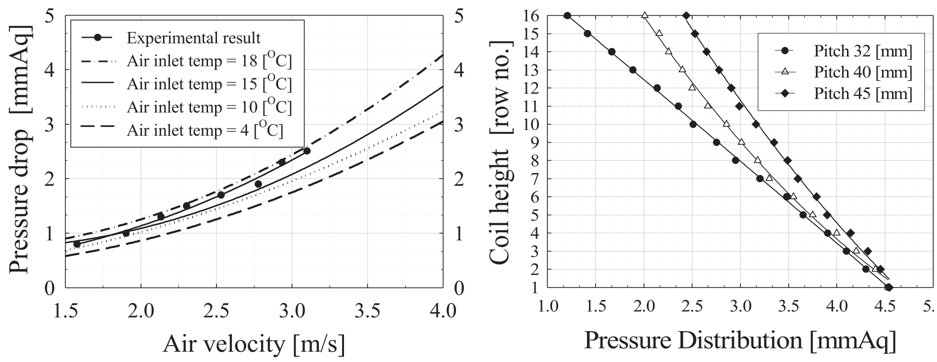

(a) (b)

Fig. 2. Pressure drop w.r.t. air inlet velocity (a); w.r.t. coil pitch (b).

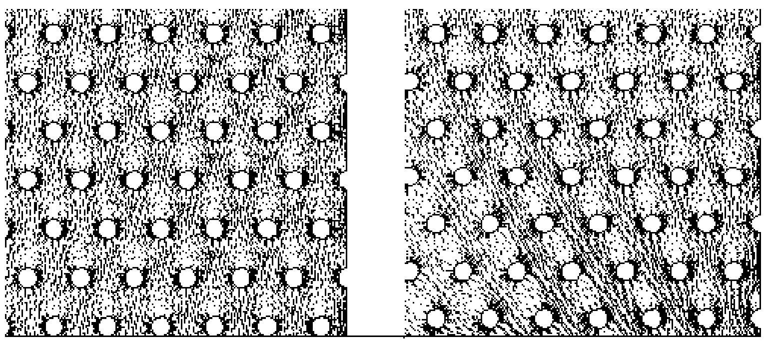

(a) (b)

Fig. 3. Predicted air flow for air supply from (a) bottom; (b) side wall.

The temperature distribution along the coil height for air supply from both the side wall and from the bottom end is shown at the left panel in Fig. 4. The temperature drop at the first five to six rows are seen to be sharper than other for both cases. The wakes shed by the first row produce a high level of free stream turbulence for the second row of tubes, thereby increasing the heat transfer coefficient for the second row. This effect moderates after about the fifth row in the coil bank, so the heat transfer coefficients for tubes beyond the fifth row seems to differ little. The range of temperature, calculated subtracting the temperature of the bottom row from the top one, was about $1.4\,^{\circ}\mathrm{C}$ for the air supply from the bottom and was about $1.17\,^{\circ}\mathrm{C}$ for the air supply from the side wall. Therefore, the cooling capacity of the HCCCT having air supply from the bottom end for the dry mode operation was 33.6 Mcal/h (39 kW in SI). This capacity could be compared to the measured capacity of 32 Mcal/h (37 kW).

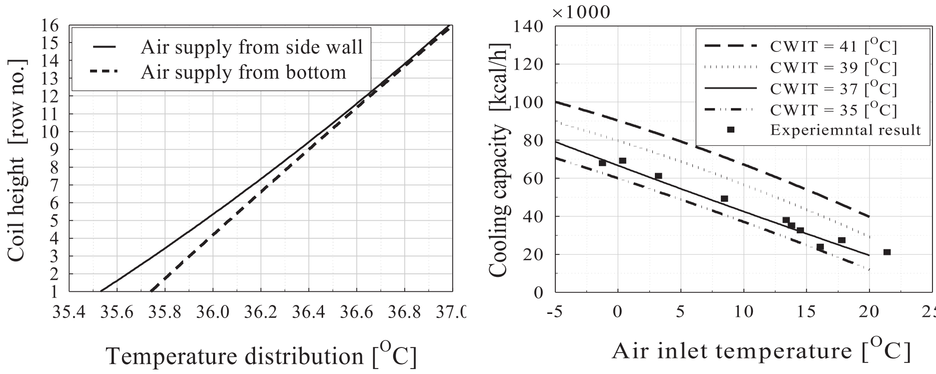

(a) (b)

Fig. 4. Temperature distribution w.r.t. air inlet location (a); cooling capacity w.r.t. air inlet temperature (b).

For the dry mode, the cooling capacity depends on the inlet temperatures of the cooling water and the surrounding air. The effects of air inlet temperature having different Cooling Water Inlet Temperature (CWIT) ranging from 35–41 °C were investigated. The comparative cooling capacities are shown at the right panel of Fig. 4. The cooling capacities were found to increase drastically with the decrease of the air inlet temperature. The increasing CWIT augmented the increase of the cooling capacity as well. Although cooling capacity can be increased with higher CWIT, the outlet cooling water temperatures in such cases are also high which is undesirable. The experimental cooling capacity which is measured at a bit different range was found to conform well to the numerically calculated one.

Performance of the HCCCT can be substantially improved if spray water is used along with the air from the bottom and this aspect is discussed next.

5.2 The wet mode operation

The predicted trajectories of the water droplets inside the HCCCT are shown in Fig. 5, where the left panel shows the injection of the spray water from 3 nozzles and the right panel gives a clearer view of the bouncing pattern of the single droplet trajectory which bounces several times before reaching the water basin. In wet mode, the temperature drop of the cooling water flowing inside the coil mainly depends on the air wet-bulb temperature and the spray water temperature followed by the flow rates of the cooling water and the spray water as discussed next.

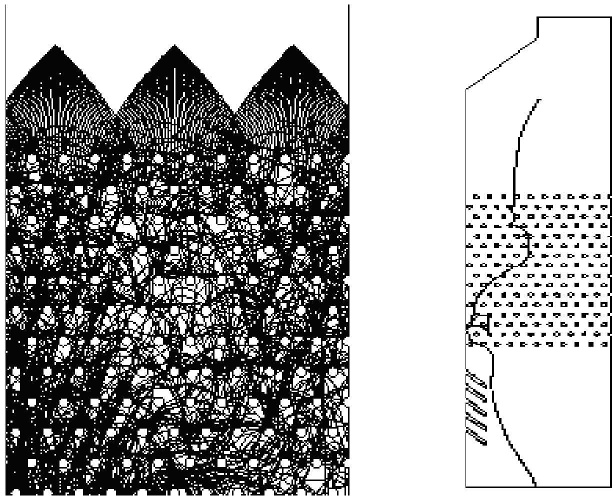

(a) (b)

Fig. 5. Injection from 3 nozzles (a); single particle trajectory (b).

5.2.1 The temperature drop of the cooling water with respect to wet-bulb temperature

The cooling capacity has been investigated for WBT of 24, 27 and $30\,^{\circ}$C and the comparative temperature distribution is shown in Fig. 6, where the temperature is found to decrease with the increase of the WBT and vice versa. At the nominal operation condition, i.e. at a WBT $27\,^{\circ}$C, the predicted temperature difference from the top row to the bottom is about 4.85, therefore, the cooling capacity of HCCCT was found to be 29.8 RT (104.8 kW) which compares well with the measured capacity of 29.7 RT (104 kW).

5.2.2 The cooling capacity w.r.t. cooling water to air mass flow rates

The temperature drop as well as the cooling capacity of the HCCCT largely depends on the mass flow rates of the cooling water (W), air (G) and the spray water (L). Fig. 7 shows the cooling capacity with regard to the cooling water to air mass flow rates for different spray water volume flow rates. It may be mentioned that, the air mass flow rates is kept constant at the simulation condition. Spray water flow rates of 25–37 m^3/h are studied and found that, the cooling capacity increases with the increase of the cooling water flow rates and spray water flow rates. The flat pattern of the curves indicates that the increasing rate of the cooling capacity for the higher cooling water flow rate is rather slow and for the W/G ratio greater than 0.8, there is no appreciable increase of the cooling capacity for any further increase of the cooling water flow rate. It may also be noted that the rate of the increase of the cooling capacity becomes slower with the increase of the spray water volume flow rate. This could be due to the fact that when the spray water flow rate increases excessively, the evaporation of the water droplet at the contact surface of the coil bank can't continue that smoothly. For the spray water flow rate of $33\ \mathrm{m^3/h}$ and at $\mathrm{W/G} = 0.8$, the cooling capacity was calculated to be 29.5 RT (103.7 kW) which conforms well to the measured capacity.

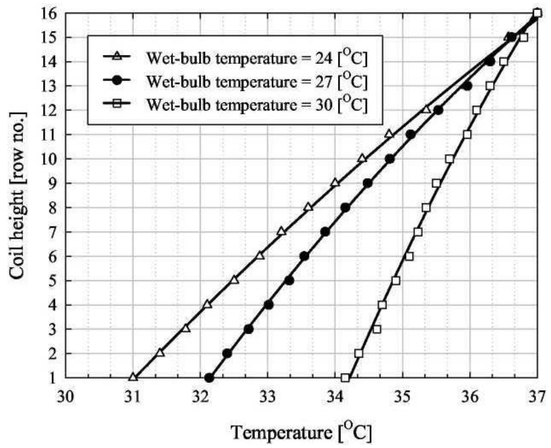

Fig. 6. Temperature drop along coil height w.r.t. wet-bulb temperature.

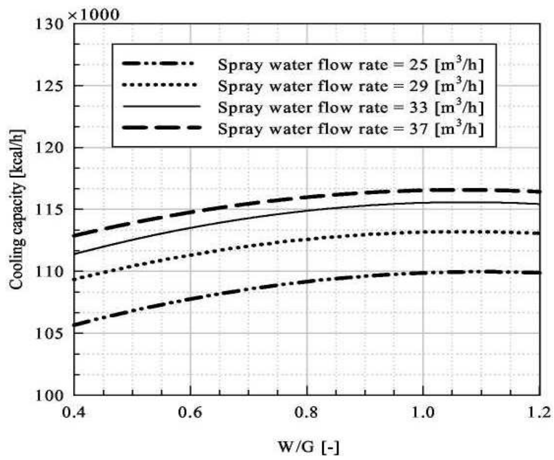

Fig. 7. Cooling capacity w.r.t. cooling water to air mass flow rate for different spray water volume flow rates.

5.2.3 Pressure drop with respect to air inlet velocity

Fig. 8 shows the pressure distribution with respect to air velocity. It's evident that the pressure decreases almost exponentially with the increasing air velocity along the height of the coil. At the nominal simulating condition, the pressure drop was around 4.11 mmAq which can be compared to the experimental pressure drop of 3.9 mmAq.

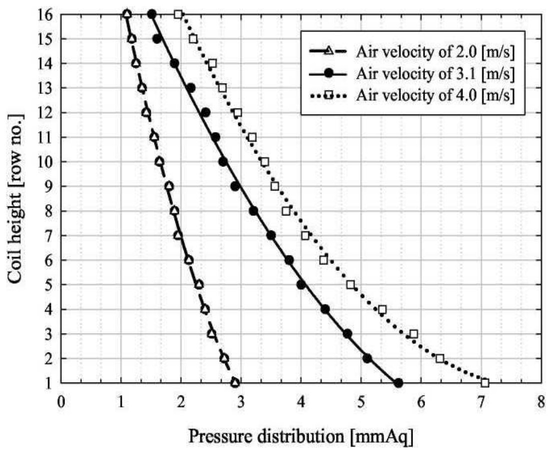

Fig. 8. Pressure drop along the coil height by air inlet velocity.

6 Conclusions

The numerical simulation of the performance characteristics of the HCCCT has been studied in this paper. Different coil pitches, cooling water flow rates, spray water flow rates and air inlet velocity and temperature have been investigated for devising the optimum designed HCCCT so that air and water consumption as well as initial and operational cost can be minimized. Characteristics have also been investigated having the air inlet at the side wall as well as at the bottom end for the dry mode and found that both pressure drop and the cooling capacity conformed well with the experimental result for the air supply from the bottom which facilitated a uniform air distribution over the coil bank. Cooling capacity for dry mode was studied with respect to air inlet temperature for different air inlet velocity and noted that the capacity increased remarkably with the decrease of the air inlet temperature. The maximum cooling capacity of the HCCCT in dry mode-winter operation was 39kW which conformed well to the experimental capacity. This CFD simulation indicated that pressure drop in a HCCCT can be affected by the coil's pitch, air inlet velocity, location of the air inlet and spray water flow rates. In wet mode operation, cooling capacity and pressure drop was investigated having air supply from the bottom end only. The cooling capacities in wet mode were studied with respect to WBT, flow rates of cooling water, spray water and air. The maximum capacity in wet mode was 104.8 kW that was also in good agreement with the experimental capacity once again. It may be mentioned that the increasing rate of the cooling capacity slowed down perceptibly for the very high flow rates. The current study demonstrated that if the simplifications made for the sake of simulation are applied sensibly and the counterbalance for that are done properly, then a CFD package can be utilized to predict the performance characteristics of HCCCT.

Acknowledgement

This study was supported financially by the Regional Industrial Technology Development Program, 2003, Pukyong National University, South Korea. The cooperation is greatly appreciated.

References

1. B. Korenic, *Computerized Simulation of Closed Circuit Cooling Towers with Parallel and Counterflow Spray Water-Air Flow Design*, TP95-17, 1995.

2. GEA erge-spirale soramat, `http://www.gea-erge.fr/`.

3. W. H. Walker, W. K. Lewis, W. H. McAdams, E. R. Gilliland, *Principles of Chemical Engineering*, 3rd ed., New York, McGraw-Hill Inc, 1923.

4. F. Merkel, Verdunstungskuehlung, VDI Forschungsarbeiten, no. 275, Berlin, 1925.

5. S. P. Fisenko, A. I. Petruchik, A. D. Solodukhin, Evaporative cooling of water in a natural draft cooling tower, *International Journal of Heat and Mass Transfer*, **45**(23), pp. 4683–4694, 2002.

6. J.-U.-R. Khan, S. M. Zubair, An improved design and rating analyses of counter flow wet cooling towers, *ASME Journal of Heat Transfer*, **123**(4), pp. 770–778, 2001.

7. A. Hasan, G. Gan, Simplification of analytical models and incorporation with CFD for the performance predication of closed-wet cooling towers, *International Journal of Energy Research*, **26**(16), pp. 1161–1174, 2002.

8. H. Jaber, R. L. Webb, Design of cooling towers by the effectiveness-NTU method, *ASME Journal of Heat Transfer*, **111**(4), pp. 837–843, 1989.

9. T. Mizushina, R. Ito, H. Miyashita, Experimental study of an evaporative cooler, *International Chemical Engineering*, **7**(4), pp. 727–732, 1967.

10. G. Gan, S. B. Riffat, Numerical simulation of closed wet cooling towers for chilled ceiling systems, *Applied Thermal Engineering*, **19**(12), pp. 1279–1296, 1999.

11. G. Gan, S. B. Riffat, L. Shao, P. Doherty, Application of CFD to closed-wet cooling towers, *Applied Thermal Engineering*, **21**(1), pp. 79–92, 2001.

12. G. Gan, S. B. Riffat, L. Shao, Performance prediction of a prototype closed wet cooling tower, *Journal of the Institute of Energy*, **73**(495), pp. 106–113, 2000.

13. Daeil Aqua Co. Ltd., `http://www.daeilaqua.com/`.

14. FLUENT, User's Guide, Fluent Inc., Lebanon, NH 03766, 2005.

15. J. P. Van Doormal, G. D. Raithby, Enhancements of the simple method for predicting incompressible fluid flows, *Numerical Heat Transfer*, **7**(2), pp. 147–163, 1984.

16. S. P. Fisenko, A. A. Brin, A. I. Petruchik, Evaporative cooling of water in a mechanical draft cooling tower, *International Journal of Heat and Mass Transfer*, **47**(1), pp. 165–177, 2004.

17. V. G. Levich, *Physicochemical Hydrodynamics*, Prentice-Hall, NJ, 1962.